INTERNATIONAL JOURNAL OF PLANT BASED PHARMACEUTICALS

RESEARCH ARTICLE

OPEN ACCESS

Docking-based virtual screening, ADMET, and network pharmacology prediction of anthocyanidins against human alpha-amylase and alpha-glucosidase enzymes as potential antidiabetic agents

Cihan Demir[a] [iD], Erman Salih Istifli[b*] [iD]

ª Kilis 7 Aralik University, Graduate Education Institute, Department of Molecular Biology and Genetics, TR-79000, Kilis, Turkey
ᵇ Cukurova University, Faculty of Science and Literature, Department of Biology, TR-01330, Adana, Turkey

ARTICLE INFO

ABSTRACT

Diabetes mellitus (DM) characterized by high blood sugar concentration is a major global public health problem and untreated DM results in blindness, kidney failure, heart attack, stroke, and lower extremity amputation. In this structure-based drug design (SBDD) study, the potential inhibitory effects of twelve anthocyanidins (aglycon unit of anthocyanins) components on human pancreatic α-amylase and intestinal α-glucosidase enzymes were investigated using the molecular docking method and a novel approach developed by our research group was used to rank the global binding potentials of ligands to a series of different enzymes simultaneously. In addition, drug-likeness, absorption-distribution-metabolism-excretion-toxicity (ADMET) predictions, and intracellular target-component interaction network analyses of twelve anthocyanidin components were performed using the search tool for interactions of chemicals (STITCH). Petunidin, peonidin, and aurantinidin were determined as 'hit' phytochemicals according to the docking binding energy and relative binding capacity index (RBCI) analyses, whereas, based on the RBCI index, petunidin was found to be the most effective ligand in terms of binding capacity to both enzymes that play an important role in DM. The more accessible and large-volume active site of α-amylase compared to α-glucosidase caused petunidin to bind with higher affinity against α-amylase. Promisingly, petunidin did not violate any of the criteria for drug-likeness consisting of a combination of the Lipinski's rule of 5, Ghose and Veber filters, showed no cytochrome (CYP) P450 or hERG I-II inhibitory activity in the ADMET analysis, however, it was found to have a low gastrointestinal absorption profile. In intracellular target-component network analysis using the STITCH online platform, it was determined that petunidin did not show negative functional interactions with any enzyme in the human protein network. Considering these results, it is recommended that petunidin be advanced to further *in vitro* and *in vivo* assays as a potential α-amylase and α-glucosidase inhibitory agent in the treatment of DM. However, the intestinal absorption profile of petunidin must be enhanced by molecular optimization without compromising its pharmacological activity.

List of Abbreviations

DM	: Diabetes mellitus
SBDD	: Structure-Based Drug Design

RBCI	: Relative Binding Capacity Index
ADMET	: Absorption-Distribution-Metabolism-Excretion-Toxicity
STITCH	: Search Tool for Interactions of Chemicals
CYP	: Cytochrome
IDF	: International Diabetes Federation
GDM	: Gestational Diabetes mellitus
T2DM	: Type 2 Diabetes mellitus
DFT	: Density Functional Theory
B3LYP	: Becke, 3-parameter, Lee–Yang–Parr
ATB	: Automated Topology Builder
PDB	: Protein data bank
NAMD	: Nanoscale Molecular Dynamics
Ro5	: Lipinski's rule of 5

ClogP   : Consensus octanol-water partition coefficient
Caco-2   : Caucasian colon adenocarcinoma cell line
VDss   : Steady-state volume of distribution
logBB   : Logarithmic ratio between the concentration of a compound in the brain and blood
logPS   : The blood-brain permeability-surface area product
BBB   : Blood Brain Barrier
CNS   : Central Nervous System
OCT2   : Renal organic cation transporter 2
pkCSM   : Predicting small-molecule pharmacokinetic properties using graph-based signatures
MRTD   : Maximum recommended tolerated dose
hERG   : Human ether-a-go-go gene
LD_{50} : Lethal dose 50
LOAEL   : Lowest observed adverse effect level
$pIGC_{50}$: Negative logarithm of the concentration required to inhibit 50% growth in log µg/ml
LC_{50} : Lethal concentration 50

1. Introduction

Diabetes mellitus (DM) is a chronic metabolic disorder and is diagnosed with an elevated glucose concentration in the blood above the basal level. Among the clinical signs of DM, insulin secretion is observed to be generally defective, and the peripheral effects of insulin are weakened. In addition, defective metabolism of lipids, proteins, mineral salts, or electrolytes may accompany DM (Pérez Gutierrez et al., 2006). The International Diabetes Federation (IDF) reported that approximately 415 million adults aged 20 to 79 years had diabetes in 2015 (Zheng et al., 2018). This number, which is expected to increase by 200 million by 2040, is predicted as a global public health burden (Zheng et al., 2018). Although chronic hyperglycemia in DM patients causes damage to various organ systems, the most prominent of these are micro and macrovascular complications that increase cardiovascular risk. The incidence of DM is increasing globally due to the increase in lifestyles within the framework of unhealthy living conditions (obesity, wrong eating habits, physical inactivity, alcohol consumption, or smoking) (Chen et al., 2012; Forouhi and Wareham, 2014). The most prominent evidence that DM increases with age are that approximately 25% of the population over 65 years of age has diabetes (Carrillo-Larco et al., 2019).

Based on etiology and clinical findings, DM is classified into three categories: type 1 diabetes, type 2 diabetes, and gestational diabetes (GDM). Type 2 diabetes is found in the majority (90%) of all diabetes cases (Oliveira et al., 2020). In T2DM, the effect of insulin as a glucose utilization regulator is diminished, and this medical phenomenon is termed 'insulin resistance'. In the case of insulin resistance, insulin in the organism cannot function, a situation that contradicts the increased insulin production that initially occurs to maintain glucose homeostasis. Over time, insulin production decreases and T2DM develops. The prevalence of DM is most common in people older than 45 years. However, due to increasing obesity, physical inactivity, and energy-dense diets, DM has been increasingly diagnosed in children, adolescents, and young adults (Oliveira et al., 2020).

Phytochemicals offer a unique option for the discovery of new antidiabetic compounds with fewer side effects (Jayawardena et al., 2012). In this context, the combined use of plant-based compounds containing trace elements such as chromium or zinc arouses great interest in the scientific community, because activation of certain processes in glucose homeostasis and insulin sensitivity (activation of insulin receptor signaling pathway by chromium, the antioxidant activity of selenium and zinc) or enzymatic inhibition (inhibition of phosphatases by selenium) is thought to be promising (Wiernsperger and Rapin, 2010).

Therefore, various alkaloids, phenolic compounds, saponins, polysaccharides, terpenoids, glycosides, and xanthones that people take into the body by consuming different foods are important bioactive compounds (Coman et al., 2012).

Anthocyanins, a subcategory of dietary flavonoids, are water-soluble pigments that produce quite different colors (red, pink, purple, orange, and blue) in plants, fruits, vegetables, and leaves (Castañeda-Ovando et al., 2009; Wallace and Giusti, 2015). Anthocyanins are abundant in many vegetables, fruits, and tuber-type metamorphic vegetables (Belwal et al., 2017). Furthermore, anthocyanin content and composition vary widely in plant foods, especially fruits with high anthocyanin concentrations (Horbowicz et al., 2008). Anthocyanidins, aglycone forms of anthocyanins, are structured based on the 2-phenylbenzopyrilium or flavylium ions and carry methoxy or hydroxyl groups at different positions (Sivamaruthi et al., 2018). The human diet contains six major anthocyanidins (aglycone unit of anthocyanins), cyanidin, delphinidin, malvidin, pelargonidin, peonidin, and petunidin, however, there are also anthocyanidins such as aurantinidin, capensinidin, europinidin, hirsutidin, pulchellidin, and rosinidin identified in nature. Color is a general property of anthocyanins/anthocyanidins and research indicates that it can be important in dietary guidance as certain anthocyanins/anthocyanidins and/or their metabolites have specific effects in reducing the risk of T2DM (Liu et al., 2022; Peterson et al., 2015; Zamora-Ros et al., 2011).

In this study, it was aimed to investigate the inhibitory potentials of certain anthocyanidin molecules (aurantinidin, capensinidin, cyanidin, delphinidin, europinidin, hirsutidin, malvidin, pelargonidin, peonidin, petunidin, pulchellidin, and rosinidin) (Figure 1) commonly found in plants on human pancreatic α-amylase and intestinal α-glucosidase (maltase glucoamylase) using the molecular docking method. Furthermore, drug-likeness properties, ADMET profiles, and *Homo sapiens* component-target interaction network of these compounds were also determined. It has been suggested that the hit anthocyanidin compounds that we determined in this study may be advanced to preclinical *in vitro* and *in vivo* studies to accelerate DM treatment.

2. Materials and methods

2.1. Structural optimization of ligands

Before molecular docking studies, the geometric optimization of 12 anthocyanidin molecules (ligands) was performed on the Automated Topology Builder (ATB) server (https://atb.uq.edu.au/) using the density functional theory (DFT/B3LYP/6-31G* basis set). After the geometry optimization of ligands, the energetically optimized 3D structures calculated by the ATB server were saved in pdb (protein data bank) file format before submission to molecular docking simulations (Malde et al., 2011).

2.2. Retrieval of α-amylase and α-glucosidase proteins and their structural optimization using nanoscale molecular dynamics (NAMD)

In the current study, the X-ray crystal structures of human α-amylase (PDB ID: 1B2Y) and α-glucosidase (maltase glucoamylase) (PDB ID: 3TOP) are downloaded from the Protein Data Bank (https://www.rcsb.org/) (RCSB PDB). Water molecules, co-

crystallized ligands, and non-interacting ions were removed from the protein structures before docking. Before energy minimization with NAMD (Nanoscale Molecular Dynamics), missing amino acid side chains and hydrogen atoms of protein molecules were added using the UCSF Chimera program. Then, in the Vega ZZ program, pancreatic α-amylase was ionized at pH 7.0, whereas the intestinal α-glucosidase was ionized at pH 5.0 (Sky-Peck and Thuvasethakul, 1977; Tomasik and Horton, 2012). In protein-energy minimization with NAMD, the atom types and electrical charges of the enzymes were fixed in the Vega ZZ program using the CHARMM22_PROT

force field and Gasteiger-Marsili charges (Pedretti et al., 2004). Then, parameters required for energy minimization of proteins were loaded from a template file in the NAMD module of the same software. The value 10.000 was determined as the number of time steps, and the CHARMM22_PROT as the force field. Following the energy minimization, the lowest energy conformers (the last minimization step) of both proteins were recorded in protein data bank (pdb) format.
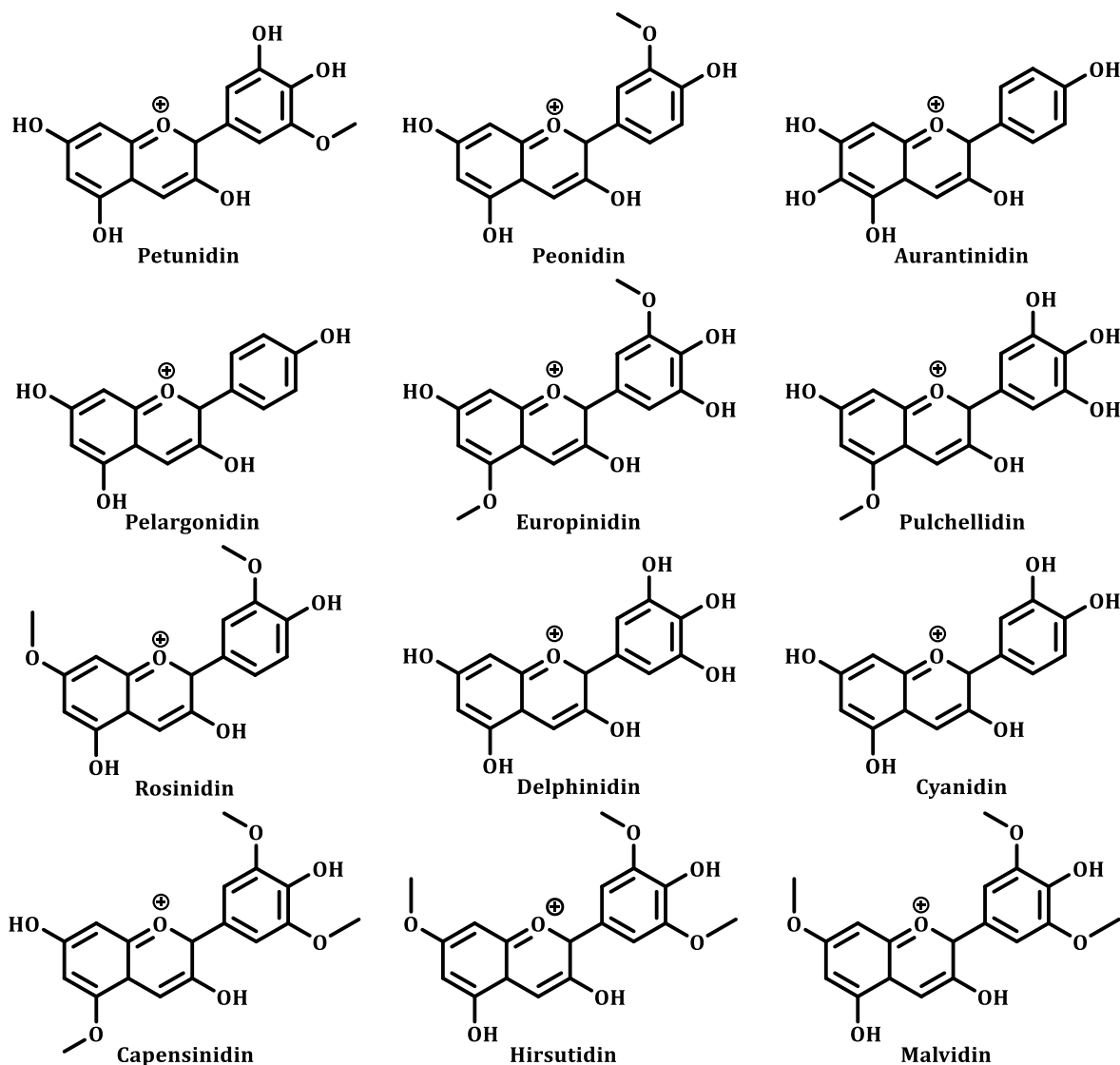

Figure 1. Chemical structures of anthocyanidins

2.3. Molecular docking

Molecular docking simulations between α-amylase and α-glucosidase (maltase glucoamylase) enzymes and anthocyanidins were performed using AutoDock Vina 1.2.0 program (Trott and Olson, 2010). In this rigid receptor-flexible ligand docking protocol, the binding affinity and binding conformations of anthocyanidins against the active sites (inhibitor binding site) of α-amylase and α-glucosidase enzymes were predicted with the AutoDock Vina 1.2.0 program. The AutoDockTools-1.5.6 interface has been used to prepare receptors and ligands before molecular docking experiments (Sanner, 1999). In molecular docking studies, the

coordinates of the search spaces of the protein active sites were determined to allow ligands to interact easily with these regions. The determination of the active sites of α-amylase and α-glucosidase was performed using the cartesian coordinates of the bound experimental inhibitor (acarbose).

Using this approach, α-amylase active site coordinates were set as, x: 18.90, y: 5.79, z: 47.00 (size x: 28; size y: 28; size z: 28), and the α-glucosidase active site were set as, x: -55.97, y: 8.45, z: -64.73 (size x:30; size y:30, size z:30) accordingly.

After a total of 20 independent docking runs for each anthocyanidin, all possible ligand conformations were clustered by AutoDock Vina 1.2.0 according to geometric similarity and ranked based on the most favorable (negative) binding free energy (kcal/mol). Top-ranked poses of receptor-ligand complexes obtained with AutoDock Vina 1.2.0 were visualized using BIOVIA DS Visualizer v16 and examined for anthocyanidin-amino acid non-bonded interactions.

2.4. Determination of the relative binding capacity index (RBCI) of phytochemicals

In this study, 'Relative Binding Capacity Index (RBCI)' analysis, which is a new approach in the literature and enables a more efficient ranking of different ligands in molecular docking based on the receptors to which they show affinity, was performed (Istifli et al., 2022). RBCI provides a comparison of statistically relevant data that can have different scientific meanings. Because the binding affinities of ligands are different for each protein, phytochemicals can only be evaluated based on their potency in that parameter, if they are ranked in the light of their binding energies to a single protein. However, ranking based on only one of the receptors may not fully represent the activity potentials of the ligands. One of the most common methods used to rank interactions between receptor and ligand is to calculate the 'central bias'. In this method, ligands (components) are ranked based on the average value of their affinity for all receptors. If the values (binding free energy) in each data set are converted into standard scores, it is possible to compare these values with each other. Therefore, in this study, arithmetic mean and standard deviation were obtained for each protein by using binding free energy values of ligands. The raw standard scores were obtained by subtracting the binding free energy values of each ligand for each protein from this arithmetic mean and then dividing by the standard deviation value (see equation given below) (Sharma, 1996). The RBCI values of the ligands were obtained by calculating the averages of the standard scores (for each protein) as described above.

$$Standard\ score = (x-\mu)/\sigma$$

In the formula, 'x' stands for raw data, 'μ' stands for mean and 'σ' stands for standard deviation. Although RBCI is a relative value and does not fully represent the specific binding capacity of ligands, it makes possible to acceptably rank ligands according to their binding free energy values against all target receptors. Thus, RBCI could be viewed as an integrated approach to statistically rank order ligands based on their molecular interactions with different receptors since it considers the binding affinity for all receptors simultaneously.

2.5. Drug-likeness and absorption-distribution-metabolism-excretion-toxicity (ADMET) prediction

Determination of drug similarity (drug-likeness) and ADMET (absorption-distribution-metabolism-excretion-toxicity) profiles of promising hit compounds in structure-based drug design (SBDD) studies is important in terms of reducing their side effects on the target organism. In this work, SwissADME and pkCSM platforms were employed to predict drug-likeness and ADMET properties of anthocyanidins, for which docking simulations were performed against α-amylase and α-glucosidase enzymes (Daina et al., 2017; Daina et al., 2019; Pires et al., 2015).

2.6. Network pharmacology analysis

In the drug discovery process, the single drug/single target approach has some shortcomings in terms of safety and effectiveness (Chandran et al., 2015). Therefore, the application of a network pharmacology approach is necessary and inevitable in predicting the interactions of small molecules with the protein network of the relevant organism, revealing possible side effects of 'hit' or 'lead' compounds, or in the elucidation of novel therapeutic effects. In our study, component-target analysis of anthocyanidin molecules, which were determined as 'hit' according to the RBCI analysis, was performed using the STITCH (http://stitch.embl.de/) platform where 'H. sapiens' was selected as the target organism.

3. Results and discussion

In this computational virtual screening study, the inhibitory potentials of twelve naturally occurring anthocyanidins (aglycone units of anthocyanins) (Table 1) against human pancreatic α-amylase and intestinal α-glucosidase (maltase-glucoamylase) enzymes were investigated using molecular docking method. The binding free energy (ΔG° = kcal/mol) calculated as a result of molecular docking was used as a criterion in the evaluation of the inhibition potentials of anthocyanidins on these enzymes.

Table 1. PubChem CID, molecular weight, and molecular formulas of anthocyanidins

No	Molecule	PubChem CID	Molecular weight (g/mol)	Molecular formula
1	Aurantinidin	441648	287.24	$C_{15}H_{11}O_6^+$
2	Capensinidin	441658	345.30	$C_{18}H_{17}O_7^+$
3	Cyanidin	128861	287.24	$C_{15}H_{11}O_6^+$
4	Delphinidin	68245	338.69	$C_{15}H_{11}ClO_7$
5	Europinidin	14496547	331.30	$C_{17}H_{15}O_7^+$
6	Hirsutidin	441694	345.30	$C_{18}H_{17}O_7^+$
7	Malvidin	159287	331.30	$C_{17}H_{15}O_7^+$
8	Pelargonidin	440832	271.24	$C_{15}H_{11}O_5^+$
9	Peonidin	441773	301.27	$C_{16}H_{13}O_6^+$
10	Petunidin	73386	352.72	$C_{16}H_{13}ClO_7$
11	Pulchellidin	14496545	317.27	$C_{16}H_{13}O_7^+$
12	Rosinidin	441777	315.30	$C_{17}H_{15}O_6^+$

Source: https://pubchem.ncbi.nlm.nih.gov/

Anthocyanidins structurally originate from the flavylium cation, an oxonium ion ($C_5H_5O^+$), and the hydrogen atoms in their structures are replaced by various functional groups (Figure 2). Generally, the colors they carry as a function of ambient pH can change from red to purple, blue, or bluish green (Iacobucci and Sweeny, 1983; Khoo et al., 2017). Furthermore, anthocyanidins are an important subclass of polymethine dyes and flavonoids. The flavylium cation is a chromium cation with a phenyl group attached to the 2nd carbon atom, and chromenillium (also known as benzo pyrylium) is a bicyclic version of pyrylium. The positive charge can move around the molecule (Khoo et al., 2017) (Figure 2).

3.1. RBCI values and molecular docking binding energies of anthocyanidins

Molecular docking is a structure-based drug design method (Structure-Based Drug Design = SBDD) that predicts the energetically lowest energy binding conformation of small molecule ligands on the target protein (receptor) (Dos Santos et al., 2018; Meng et al., 2011).

Molecular simulations, in this work, were performed between receptor molecules (pancreatic α-amylase and intestinal α-glucosidase) and 12 anthocyanidin components (aurantinidin, capensinidin, cyanidin, delphinidin, europinidin, hirsutidin, malvidin, pelargonidin, peonidin, petunidin, pulchellidin, and rosinidin), and

the binding free energy (ΔG° = kcal/mol) of each anthocyanidin ligand against the target proteins was calculated. The obtained top-ranked conformations of anthocyanidins were saved and the chemical bonds stabilizing the resulting protein-ligand complexes were characterized. As a result of the RBCI analysis (Figure 3), that was performed using the binding free energy values of the ligands for both enzymes, it was determined that the 'hit' ligands among the 12 anthocyanidins were petunidin, peonidin, and aurantinidin. Therefore, the docking results of petunidin, peonidin, and aurantinidin were discussed in this section. The docking binding free energies and inhibition constants (K_i) of petunidin, peonidin, and aurantinidin are given in Table 2.
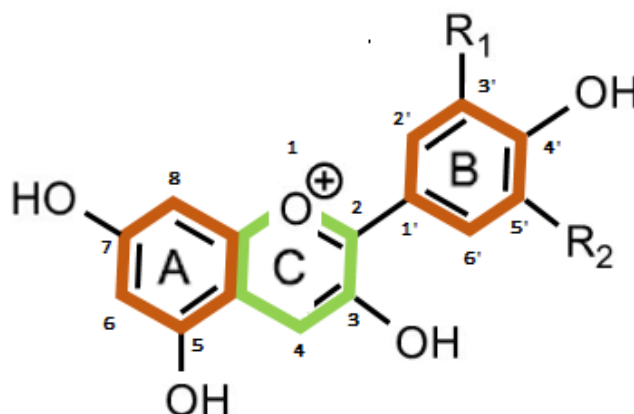

Figure 2. Structure of an anthocyanidin molecule.
The orange-colored aromatic rings are benzene (A and B), and the green-colored aromatic ring (C) is the pyrylium ring.
Anthocyanidins are named according to the specific groups at the R_1 and R_2 positions on the B ring
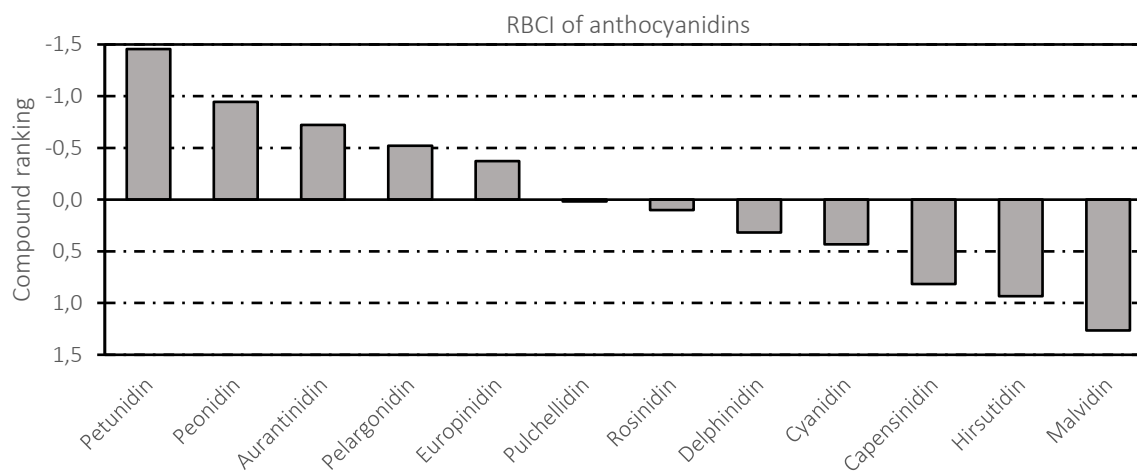

Figure 3. RBCI calculated using the binding free energy (kcal/mol) values of anthocyanidins against α-amylase and α-glucosidase enzymes.
The increase in the negative value of RBCI indicates that the compound in question binds more strongly with the active sites of both target receptors (α-amylase and α-glucosidase).

According to Table 2, while peonidin showed the highest affinity for the pancreatic α-amylase enzyme (ΔG°= -8.16 kcal/mol), petunidin (ΔG°= -7.37 kcal/mol) was determined to be the most effective ligand against intestinal α-glucosidase. K_i values of petunidin, peonidin, and aurantinidin molecules were determined to be between 0.90 − 1.60 μM for α-amylase, and 3.70 − 9.50 μM for α-glucosidase, respectively. Given that a drug candidate hit compound typically exhibits activity at concentrations close to 1 μM (Krasiński et al., 2005; Pellecchia et al., 2004), the binding affinity values of petunidin, peonidin, and aurantinidin molecules to the active site of

the pancreatic α-amylase, in particular, are promising (Table 2). One of the most likely reasons for the stronger binding of these 3 phytochemicals to α-amylase compared to α-glucosidase is that the solvent-exposed surface of the α-amylase active site is conformationally larger in volume and more accessible. To examine this structural difference between the two enzymes, the inhibitor binding sites of human α-amylase (PDB ID:1b2y) and α-glucosidase (PDB ID:3top) can be visualized in the RCSB PDB database.

Table 2. Binding free energy (ΔG°=kcal/mol) and inhibition constant (K$_i$: μM) values of the interaction between hit anthocyanidins and human pancreatic α-amylase and intestinal α-glucosidase (maltase-glucoamylase) enzymes

No	Molecule	Enzyme	Binding free energy (kcal/mol)	Inhibition constant (K$_i$=μM)	Enzyme	Binding free energy (kcal/mol)	Inhibition constant (K$_i$=μM)
1	Petunidin	α-Amylase	-7.86	1.60	α-Glucosidase	-7.37	3.70
2	Peonidin	α-Amylase	-8.16	0.90	α-Glucosidase	-6.82	9.50
3	Aurantinidin	α-Amylase	-7.92	1.50	α-Glucosidase	-7.02	6.80

3.2. Molecular interactions between hit anthocyanidins and target proteins

The intermolecular interactions of 'hit' anthocyanidins (petunidin, peonidin, and aurantinidin) with α-amylase and α-glucosidase enzymes are given in Table 3. Analysis and visualization were performed with Discovery Studio Visualizer v16 (Accelrys) software, and non-covalent interactions between hit anthocyanidins and target enzymes, as well as interacting key amino acid residues were determined (Figures 4, 5, and 6).

Table 3. Amino acid molecular contacts and chemical interactions between human pancreatic α-amylase (1B2Y) and intestinal α-glucosidase (3TOP) enzymes and top-ranked anthocyanidins

No	Molecule	Enzyme	Classical H-bond	Van der Waals	Non-classical H-bond (C-H, Pi-Donor)	Hydrophobic interaction		Electrostatic
						π-π	Mixed π/Alkyl	
1	Petunidin	α-Amylase	Gln62[1], His100[1], Asp196[1]	Trp57, Leu164[1], Arg194, Ala197, Glu232, His298, Asp299, His304[1]	-	Trp58[1], Tyr61[1]	-	-
2	Peonidin	α-Amylase	Tyr61[1]	Trp57, Gln62[1], His100[1], Leu164[1], Arg194, Asp196[1], His298, Asp299, His304	Trp58[1]	Trp58[1]	-	-
3	Aurantinidin	α-Amylase	Arg194, Asp196	Trp57, Trp58[1], Gln62, Leu161, Ala197, Glu232, His298, Asp299	-	Tyr61[1], His100[1]	Leu164[1]	Asp196[1]
1	Petunidin	α-Glucosidase	Asp198[2], Gln199[2]	Gln199, Tyr292, Trp396[2], Lys501, Phe600[2], Thr627, Ile628	-	Trp410[2], Phe601[2]	-	-
2	Peonidin	α-Glucosidase	Thr627	Asp198[2], Gln199[2], Tyr292, Trp396[2], Lys501, Ile628	-	Trp410[2], Phe601[2]	-	-
3	Aurantinidin	α-Glucosidase	Asp198[2], Thr627	Gln199[2], Pro200, Tyr292, Trp396[2], Lys501, Phe600[2], Ile628, Gly629	-	Trp410[2], Phe601[2]	-	-

[1] Active site residues of pancreatic α-amylase (PDB ID: 1B2Y) interacting with co-crystallized inhibitor (acarbose), (Trp58, Tyr61, Gln62, His100, Leu164, Asp196, Lys199, His200, Glu239, His304, Gly305)

[2] Active site residues of intestinal α-glucosidase (PDB ID: 3TOP) interacting with the co-crystallized inhibitor (acarbose) (Asp198, Gln199, Lys205, Trp396, Trp410, Phe468, Arg551, Asp567, Phe600, Phe601, Arg623, His625)

Note: In the protein preparation step using the Chimera program, the residue numbers were changed for both structures (1B2Y and 3TOP) due to the processing method of the pdb files by the DockPrep module. Thus, for the reader to find the same residues in the 1B2Y file (chain A) which are indicated in the above table for α-amylase, the number of the relevant residue should be increased by 1 (+1), and in the same way, for the 3TOP file (chain B), it is necessary to increase it by 959 (+959).

Petunidin formed H-bonds with Gln62, His100, and Asp196, π-π interactions with Trp58 and Tyr61, and many Van der Waals interactions with Trp57, Leu164, Arg194, Ala197, Glu232, His298, Asp299 and His304 of the active site of the pancreatic α-amylase (Table 3, Figure 4-A). Based on the structural analysis of the top-ranked docking pose, it could be determined that the molecular complex formed by petunidin and the α-amylase is generally stabilized by H-bonds, hydrophobic and weak electrostatic interactions. In addition, the OH groups in the A, C, and B rings of petunidin played an important role in the formation of the H-bonds (Figure 4-A).

The types of molecular interactions and top-ranked pose of petunidin in the inhibitor binding site of the human intestinal α-glucosidase enzyme are given in Table 3 and Figure 4-B, respectively. In the active site of human intestinal α-glucosidase, petunidin formed H-bonds with Asp198 and Gln199, hydrophobic π-π interactions with Trp410 and Phe601, and many Van der Waals interactions with Gln199, Tyr292, Trp396, Lys501, Phe600, Thr627 and Ile628 (Table 3, Figure 4-B). It can be inferred that the molecular complex formed between petunidin and the active site of the α-glucosidase enzyme is stabilized by H-bonds and hydrophobic interactions. The OH group on the B ring of petunidin plays an important role in the formation of H-bonds (Figure 4-B).

The types of molecular interactions of peonidin in the inhibitor binding pocket of the human pancreatic α-amylase and its top-ranked pose are given in Table 3 and Figure 5-A, respectively. Peonidin formed H-bonds and π-π interaction with Tyr61 and Trp58, and many Van der Waals contacts with Trp57, Gln62, His100, Leu164, Arg194, Asp196, His298, Asp299, and His304 within the binding pocket of human α-amylase (Table 3, Figure 5-A). It was determined that the molecular complex formed by peonidin with the active site of the α-amylase is generally stabilized by a large number of hydrophobic interactions and a small number of H-bonds. Furthermore, the OH group on the C ring of peonidin was effective in the formation of the classical H-bond (Figure 5-A).

The types of molecular interactions of peonidin in the inhibitor binding site of the human intestinal α-glucosidase and its top-ranked pose are given in Table 3 and Figure 5-B, respectively. Peonidin, within the binding pocket of α-amylase, formed H-bond with Thr627, hydrophobic π-π interaction with Trp410 and Phe601, and many Van der Waals interactions with Asp198, Gln199, Tyr292, Trp396, Lys501 and Ile628 (Table 3, Figure 5-B). It has been

determined that the molecular complex formed between peonidin and the active site of human α-glucosidase is generally stabilized by a large number of hydrophobic stacking interactions and one H-bond. The C (pyrylium) and B (benzene) rings of peonidin played an important role in the formation of hydrophobic interactions (Figure 5-B).
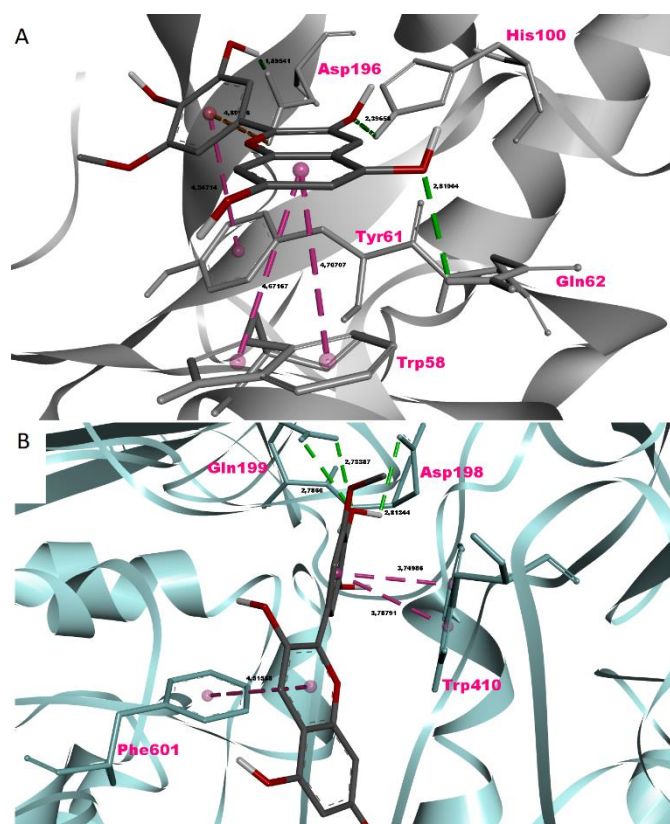

Figure 4. Top-ranked conformations of petunidin (A: α-amylase, B: α-glucosidase)

The types of molecular interactions of aurantinidin at the inhibitor binding site of the human pancreatic α-amylase and the top-ranked pose are given in Table 3 and Figure 6-A, respectively. Aurantinidin formed H-bond and electrostatic pi-anion interaction with Arg194 and Asp196, hydrophobic π-π and π-sigma contacts with Tyr61, His100, and Leu164, and many Van der Waals contacts with Trp57, Trp58, Gln62, Leu161, Ala197, Glu232, His298, and Asp299 with the α-amylase enzyme (Table 3, Figure 6-A). When the interaction of aurantinidin with the pancreatic α-amylase enzyme is examined, it is observed that the major interactions that stabilize the molecule in the active site of the enzyme are of hydrophobic type, but the H-bonds formed through the B ring also contributed to the stability of the complex (Figure 6-A).

The types of molecular interactions of aurantinidin in the inhibitor binding pocket of the human intestinal α-glucosidase and its top-ranked pose are given in Table 3 and Figure 6-B, respectively. Aurantinidin, in the active site of human intestinal α-glucosidase, formed two H-bonds with Asp198 and Thr627, hydrophobic π interactions with Trp410, Phe601, and Thr627, and numerous Van der Waals interactions with Gln199, Pro200, Tyr292, Trp396, Lys501, Phe600, Ile628, and Gly629 (Table 3, Figure 6-B). In general, it has been determined that the major interactions that stabilize aurantinidin in the active site of intestinal α-glucosidase are H-bonds and hydrophobic contacts (Figure 6-B).
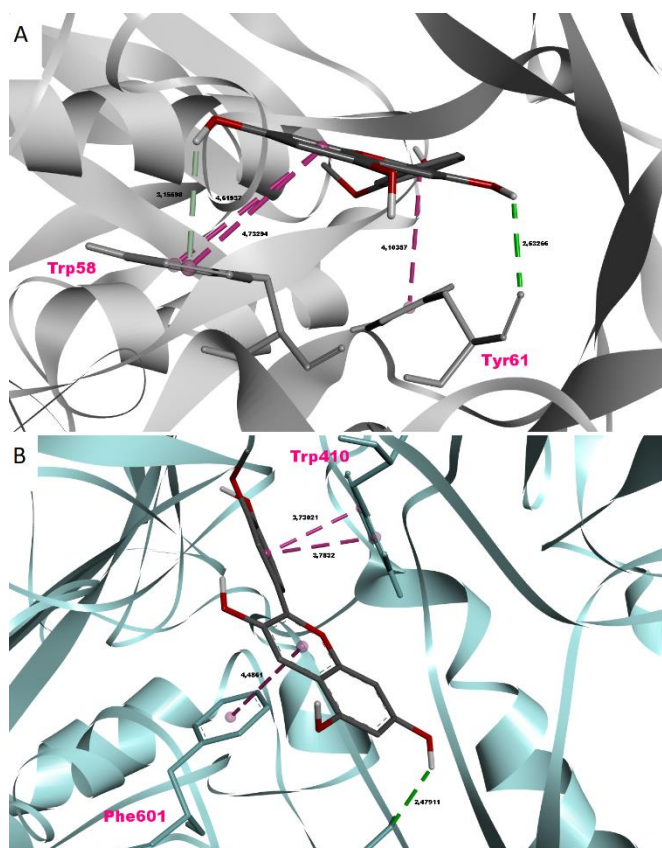

Figure 5. Top-ranked conformations of peonidin (A: α-amylase, B: α-glucosidase)

Based on a rigorous literature search, we found that there are no reports on the inhibitory potentials of petunidin, peonidin, and aurantinidin on human α-amylase or human α-glucosidase enzymes investigated by molecular docking. Therefore, our study is the first in the literature to determine the affinity between the above-mentioned ligands and human enzymes. On the other hand, since there are some docking or experimental inhibition studies of petunidin and peonidin against α-amylase or α-glucosidase enzymes obtained from non-human organisms, we compared and discussed our results with those from these studies.

It has been reported that the experimental IC_{50} value of petunidin against the α-glucosidase (maltase glucoamylase) enzyme from *Saccharomyces cerevisiae* was found to be 30.78 μM (K_i = 1.52 μM), with a mode of inhibition which was 'competitive' (Promyos et al., 2020). It was determined by the same researchers that petunidin showed a binding affinity of -7.98 kcal/mol against *S. cerevisiae* α-glucosidase enzyme in molecular docking simulations and formed non-bonded interactions with Asp327, Asp443, Asp542, and Tyr605 residues in the catalytic region of the enzyme. In general, the researchers found that the OH groups attached to the C-3', C-4', and C-5' carbons in the B ring (Figure 2) of an anthocyanidin molecule potentiate the inhibitory activity and that the OH group on the C-3' carbon of the B ring was more effective than the OH group attached to the C-5' carbon in terms of the inhibitory activity. Although the human-derived α-glucosidase enzyme was used as the target receptor in our study, petunidin interacted with Asp198 and Gln199
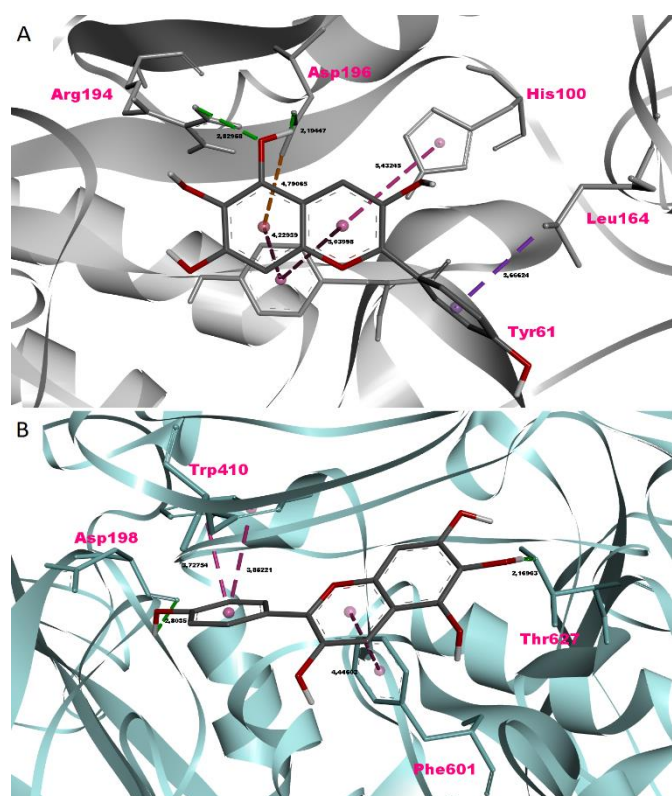
Figure 6. Top-ranked conformations of aurantinidin (A: α-amylase, B: α-glucosidase)

residues of the enzyme via the OH group attached to the C-4' carbon, but not the groups attached to the C-3' or C-5' carbons and formed 3 H-bonds (Figure 4-B). Therefore, the inhibitory reactions occurring in homologs of the same enzyme isolated from different organisms may be different, and the functional groups of the same ligand that interact with the active site residues may also differ. A low conservation value (5.34%) obtained as a result of the sequence alignment between *H. sapiens* and *S. cerevisiae* glucosidases is in line with this argument. These two homologous enzymes show great structural differences in terms of amino acid composition (Supplementary Figure S1). It has been reported that peonidin showed an IC$_{50}$ of 36.11 μM (K$_i$ = 1.23 μM) against the α-glucosidase isolated from *S. cerevisiae*, and its inhibition mode was found to be 'non-competitive' (Promyos et al., 2020). It was determined by the same researchers that peonidin displayed a binding strength of -6.40 kcal/mol against the α-glucosidase of *S. cerevisiae* in molecular docking simulations and formed chemical interactions with Asp203, Asp327, and Ser448 residues in the catalytic pocket of the enzyme (Promyos et al., 2020). In a different study, peonidin showed binding energy of -7.33 kcal/mol to the α-glucosidase enzyme isolated from the anaerobic gram-positive bacterium *Ruminococcus obeum*, and it was determined that this ligand formed chemical bonds with Asp73, Asp74, Ile76, Tyr85, Trp169, Asp197, Trp271, Asp307, Asp404, Trp417, Asp420, Lys422, and His478 residues of the enzyme (Zhang et al., 2019). In our study, peonidin formed contacts with the human α-glucosidase enzyme through residues Trp410, Phe601, and Thr627, and the C-7 carbon and B ring of the ligand (Figure 2) was effective in the formation of H-bond and hydrophobic contacts (Figure 5-B). As seen in our study and those of Zhang et al. (2019), peonidin could interact with polar and non-polar amino acid residues of α-glucosidase. Apolar (benzene and pyrylium rings) and polar (OH) functional groups of peonidin played an important role in these interactions (Figures 2 and 5-B).

Cyanidin, the other selected hit ligand in our docking study, was reported to show binding affinities of -8.18, -25.08 (*S. cerevisiae*), and -8.36 kcal/mol (*R. obeum*) against α-glucosidase enzyme isolated from *S. cerevisiae* and *R. obeum*, respectively (Chen et al., 2020; Promyos et al., 2020; Zhang et al., 2019). Delphinidin, another ligand for which docking calculations were performed in our study, has been reported to show binding capacities of -8.38 and -8.87 kcal/mol against α-glucosidase enzyme isolated from *S. cerevisiae* and *R. obeum*, respectively (Promyos et al., 2020; Zhang et al., 2019). On the other hand, malvidin and pelargonidin exhibited weak binding affinities of -3.97 and -4.69 kcal/mol against α-glucosidase enzyme isolated from *S. cerevisiae* (Promyos et al., 2020). As can be seen, cyanidin, delphinidin, pelargonidin, and malvidin, which were ranked lower according to the RBCI analysis against α-glucosidase (Figure 3), can show very high affinities against bacterial homologs of the same enzyme. However, the target enzymes (α-glucosidase and α-amylase) used in our docking study are of human origin and the amino acid residues in their catalytic sites have different characteristics in terms of both number and side chain structure (for example, the few residues in the active sites of *S. cerevisiae* α-glucosidase are predominantly composed of polar side chains, while the large number of active site residues of *H. sapiens* intestinal α-glucosidase consists of approximately equal amounts of polar and non-polar amino acids). Therefore, it was not possible to make a direct comparison with the studies of Chen et al. (2020), Promyos et al. (2020), and Zhang et al. (2019).

It has been determined that the chemical reactions of petunidin, peonidin, and aurantinidin in the catalytic sites of human α-amylase and α-glucosidase enzymes are generally stabilized by H-bonds, and a large number of hydrophobic π-π and Van der Waals interactions (Table 3). In addition, in contrast to the docking studies with *S. cerevisiae* in the literature (Promyos et al., 2020), all polar groups (-OH groups) and aromatic rings (A, C, or B) of the anthocyanidin molecule (Figure 2) play important roles to stabilize the ligand-receptor system (Figures 4, 5 and 6). In conclusion, petunidin, peonidin, and aurantinidin, which contain both polar and non-polar functional groups (Figures 1 and 2), show the ability to interact simultaneously with polar and non-polar side chains in the active sites of enzymes that play an important role in the digestive system, and therefore, they possess the ability to form stable complexes with human α-amylase and α-glucosidase enzymes.

3.3. Drug-likeness evaluation of top-ranked anthocyanidins

Drug-likeness can be defined as the molecular properties compatible with an adequate behavior in the body, namely good absorption (A), distribution (D), metabolism (M), excretion (E), and toxicity (T). Lipinski and co-workers have desired to identify, based on exclusion criteria, a formal and simplified list of molecular features that contribute most to drug similarity (Lipinski et al., 2012; Vistoli et al., 2008). In this context, 'Lipinski's rule of 5' (Ro5) attempts to elucidate broad chemical properties that can increase a molecule's chances of reaching the market (Shultz, 2018; Testa et al., 2007). On the other hand, although the popular Ro5 is quite effective in the discovery of new 'hit' or 'lead' compounds, only about 50% of chemical molecules discovered or synthesized in recent years fully comply with the Ro5 rule. In addition, some studies have shown that various organic compounds, such as macrolides and peptides, violate the chemical rules stipulated in the Ro5. Therefore, in addition to the Ro5 rule, variant filters such as the Ghose filter and the Veber rule have emerged in recent years (Congreve et al., 2003; Delaney, 2004; Ghose et al., 1999; Veber et al., 2002). Therefore, in this study, drug-likeness profiles of anthocyanidin molecules, which were docked with α-amylase and α-

glucosidase, were investigated by combining some filters such as Lipinski et al. (2012), Ghose et al. (1999), and Veber et al. (2002).

The drug similarity features of these molecules (including top-ranked petunidin, peonidin, and aurantinidin) are given in Table 4.

Table 4. Drug-likeness profiles of anthocyanidins

No	Molecule	Number of H bond acceptors	Number of H bond donors	Number of rotatable bonds	TPSA[1]	Consensus Log *P*	Log *S* (ESOL[2])	Drug-likeness (Ro5)
1	Aurantinidin	6	5	1	114.29 Å²	0.53	-3.34	Yes (0 violation)
2	Capensinidin	7	3	4	101.52 Å²	1.37	-3.80	Yes (0 violation)
3	Cyanidin	6	5	1	114.29 Å²	0.32	-2.60	Yes (0 violation)
4	Delphinidin	7	6	1	134.52 Å²	-0.98	-3.16	Yes (1 violation; NH or OH > 5)
5	Europinidin	7	4	3	112.52 Å²	1.05	-3.60	Yes (0 violation)
6	Hirsutidin	7	3	4	101.52 Å²	1.16	-3.07	Yes (0 violation)
7	Malvidin	7	4	3	112.52 Å²	0.92	-3.60	Yes (0 violation)
8	Pelargonidin	5	4	1	94.06 Å²	0.93	-3.49	Yes (0 violation)
9	Peonidin	6	4	2	103.29 Å²	0.97	-3.54	Yes (0 violation)
10	Petunidin	7	5	2	123.52 Å²	-0.31	-4.10	Yes (0 violation)
11	Pulchellidin	7	5	2	123.52 Å²	0.36	-2.66	Yes (0 violation)
12	Rosinidin	6	3	3	92.29 Å²	1.20	-3.01	Yes (0 violation)

[1] TPSA: Topological polar surface area
[2] ESOL: Estimated aqueous solubility
Web source: http://www.swissadme.ch/index.php#

When Table 4 is evaluated, the docked 12 anthocyanidin molecules show acceptable properties for a potential drug-like molecule in terms of hydrogen bond acceptor and donor numbers, rotatable bond numbers, topological polar surface area (TPSA), and consensus LogP (ClogP) values. Though only the delphinidin molecule violates the Ro5 rule in terms of H bond donor number, since the number of these violations does not exceed 1, delphinidin could also be considered a potential drug-like entity. Petunidin, peonidin, and aurantinidin, determined as top-ranked 'hit' molecules according to RBCI analysis, do not violate the Ro5 rule based on any criteria. Among these three molecules, it is observed in Table 4 that the ligand with the lowest lipophilicity (oil solubility, ClogP) is petunidin. More polar and hydrophilic compounds tend to stay in the 'liquid phase'. Therefore, considering that most of the polar drugs enter the cell via transport from various membrane-embedded proteins (Kell et al., 2011), it can be assumed that petunidin is most probably the molecule with the highest potential to enter the cell via transport proteins on the cell membrane, as petunidin showed the most negative ClogP (-0.31) value (Table 4). Besides, a low LogP value (LogP < 4) and a low molecular weight (M.W. < 400) are more suitable for ADMET parameters (Gleeson, 2008). According to previous studies, it has been observed that the LogP values of molecules with the lowest toxicity risk and optimal ADME profile vary between 2-4 at pH 7.4 (Hann and Keserü, 2012; Lobo, 2020). Therefore, petunidin has, in our opinion, an excellent ClogP (-0.31) and molecular weight (352.72 g/mol, Table 1). Therefore, the ADMET evaluations in Table 5 were performed specifically for the promising molecule, petunidin.

3.4. ADMET profile of petunidin

The extensive data owned by pharmaceutical companies can conflict with the use of Ro5 and lead to conflicting situations. Therefore, early ADMET profiling of drug candidates is a crucial factor in understanding the potential therapeutic success of a new compound and can be effective in reducing unnecessary costs when integrated into the drug development process (Vistoli et al., 2008). According to Table 5, petunidin has a good water solubility value (-2.93 log mol/l) and slightly higher solubility in water than peonidin and aurantinidin. The Caco-2 monolayer cell line is widely used as an *in vitro* model of the human intestinal mucosa for predicting the absorption of orally administered drugs (Pires et al., 2015). High Caco-2 permeability is expressed by values greater than 0.90. However, since the estimated Caco-2 permeability of petunidin is -0.19 (< 0.90), it can be said that the probability of absorption from

the human intestinal mucosa is low (Table 5). It is widely accepted that a molecule with an absorbance of less than 30% from the small intestine is poorly absorbed (Pires et al., 2015). For petunidin, this value is 68.96%, and therefore it was determined that petunidin's absorption from the small intestine is favorable (Table 5). However, considering the intestinal absorption value of other top-ranked ligand peonidin, which is 89.16%, this value (68.96%) determined for petunidin may not be reasonably high. A compound is considered to have a relatively low skin permeability if its logKp value is > -2.5. Petunidin was found to have a logKp of -2.73 (Table 5), and therefore the molecule's skin permeability is favorable. According to the calculation performed by the pkCSM online server, petunidin was determined to be a substrate of P-glycoprotein (P-gp) (Table 5). Inhibition of P-gp can increase the intracellular bioavailability of the drug molecule (Finch and Pillans, 2014). However, according to Table 5, it was also determined that the petunidin molecule was not an inhibitor of P-gp I or P-gp II. Taken together, petunidin may have the potential to be a P-gp activator. This may be an obstacle for petunidin to reach the sufficient intracellular concentration at which it can exert its pharmacological activity.

The steady-state volume of distribution (VDss) is the theoretical volume that a drug must be evenly distributed to the tissue to give the same concentration as detected in blood plasma. The higher the VD, the lower the plasma distribution of the drug, but the greater its distribution in the relevant tissue. If VDss is below 0.71 l/kg, it is considered low (log VDss < -0.15), and above 2.81 l/kg it is considered high (log VDss > 0.45) (Pires et al., 2015). In our study, the human VDss value of petunidin was determined to be 0.94. Therefore, it can be proposed that the estimated tissue distribution of petunidin is close to the baseline and possibly weak (Table 5). Associated with this data, the free fraction (fraction unbound) of petunidin in blood plasma was determined to be approximately 20% (Table 5). The ability of petunidin to cross the blood-brain barrier (BBB) was determined as -1.07 logBB (ratio of a drug's concentration in the brain to its plasma concentration), and a value less than -1 indicates that petunidin may not effectively cross the BBB (Table 5). The logPS value of petunidin was determined to be -3.88 (Table 5), indicating that the molecule could also not penetrate the central nervous system (CNS). However, the inability of petunidin to cross the BBB or CNS is not a major drawback, given that a potential anti-diabetic drug or hit molecule must act primarily on pancreatic or circulating glucose receptors.

When the estimated liver metabolism parameters of petunidin are examined, it is strikingly evident that petunidin is not a substrate or inhibitor of some cytochrome (CYP) P450 detoxification enzymes (Table 5). Not being used as a substrate by CYP enzymes indicates that petunidin is not metabolized in the liver, which is an advantageous profile for this ligand. In conclusion, petunidin, most likely, is not degraded in the liver and does not show an inhibitory effect on CYP enzymes that play a direct role in drug metabolism.

Table 5. Predicted ADMET profiles of anthocyanidins

	Model name	Aurantinidin	Capensinidin	Cyanidin	Delphinidin	Europinidin	Hirsutidin	Malvidin	Pelargonidin	Peonidin	Petunidin	Pulchellidin	Rosinidin	Unit
ABSORPTION	Water solubility	-2.96	-3.47	-2.93	-2.91	-3.22	-3.58	-3.07	-3.08	-3.05	-2.93	-2.92	-3.55	log mol/l
	Caco-2 permeability	-0.88	-0.08	-0.35	-0.32	-0.16	0.04	-0.38	-0.08	-0.13	-0.19	-1.02	0.98	log cm/S
	Intestinal absorbtion (human)	72.61	94.76	87.30	61.91	90.34	84.29	88.78	87.29	89.16	68.96	68.15	90.47	% absorbed
	Skin permeability	-2.73	-2.73	-2.73	-2.73	-2.73	-2.73	-2.73	-2.73	-2.73	-2.73	-2.73	-2.73	logK/p
	P-glycoprotein substrate	Yes	Yes	Yes	Yes	Yes	Yes	Yes	Yes	Yes	Yes	Yes	Yes	Categorical
	P-glycoprotein I inhibitor	No	No	No	No	No	No	No	No	No	No	No	No	Categorical
	P-glycoprotein II inhibitor	No	Yes	No	No	No	Yes	No	No	No	No	No	Yes	Categorical
DISTRIBUTION	[1]VDss (human)	0.84	0.54	0.95	0.96	0.66	-0.21	0.76	0.64	0.56	0.94	0.86	-0.04	log l/kg
	Fraction unbound	0.25	0.07	0.24	0.33	0.09	0.05	0.13	0.20	0.10	0.20	0.20	0.03	Fu (fraction unbound)
	BBB[2] permeability	-1.61	-1.27	-1.23	-1.28	-1.34	-1.29	-1.35	-1.06	-1.25	-1.07	-1.67	-1.19	logBB
	CNS permeability	-2.26	-3.26	-2.21	-3.92	-3.36	-3.01	-3.37	-2.02	-2.29	-3.88	-3.20	-2.21	logPS
METABOLISM	CYP2D6[3] substrate	No	No	No	No	No	No	No	No	No	No	No	No	Categorical
	CYP3A4 substrate	No	Yes	No	No	No	Yes	No	No	Yes	No	No	Yes	Categorical
	CYP1A2 inhibitor	Yes	Yes	Yes	No	Yes	Yes	Yes	Yes	Yes	No	Yes	Yes	Categorical
	CYP2C19 inhibitor	No	Yes	No	No	Yes	Yes	No	Yes	No	No	No	Yes	Categorical
	CYP2C9 inhibitor	No	No	No	No	Yes	Yes	No	No	Yes	No	No	Yes	Categorical
	CYP2D6 inhibitor	No	No	No	No	No	No	No	No	No	No	No	No	Categorical
	CYP3A4 inhibitor	No	Yes	No	No	No	No	No	No	No	No	No	No	Categorical
EXCRETION	Total clearance	0.47	0.76	0.53	0.57	0.72	0.746	0.68	0.576	0.63	0.64	0.61	0.70	log ml/min/kg
	Renal OCT2[4] substrate	No	No	No	No	No	No	No	No	No	No	No	No	Categorical
TOXICITY	AMES toxicity	No	No	No	No	No	No	No	No	No	No	No	No	Categorical
	Max. tolerated dose (human)	0.55	0.23	0.49	0.50	0.40	0.65	0.55	0.50	0.56	0.52	0.51	0.54	log mg/kg/day
	hERG I[5] inhibitor	No	No	No	No	No	No	No	No	No	No	No	No	Categorical
	hERG II inhibitor	No	No	No	No	No	No	No	No	No	No	No	No	Categorical
	Rat acute oral toxicity (LD$_{50}$)	2.49	11.72	2.46	2.54	2.34	11.72	2.34	2.43	2.40	2.45	2.54	13.91	mol/kg
	Rat chronic oral toxicity (LOAEL)	3.22	1.60	2.54	44.80	1.96	24.83	2.41	16.83	2.43	2.61	2.75	1.80	log mg/kg.bw/day
	Hepatotoxicity	No	No	No	No	No	No	No	No	No	No	No	No	Categorical
	Skin sensitization	No	No	No	No	No	No	No	No	No	No	No	No	Categorical
	T. pyriformis toxicity	0.28	0.35	0.29	0.28	0.35	0.34	0.32	0.31	0.31	0.29	0.29	0.35	log µg/l
	Minnow toxicity	1.94	1.02	2.54	31.10	2.51	1.62	1.22	1.81	1.40	3.00	2.03	1.18	log mM

[1] VDss: Volume of distribution
[2] BBB: Blood Brain Barrier
[3] CYP: Cytochrome P450
[4] OCT2: Organic Cation Transporter 2
[5] hERG I-II: Human Ether-à-go-go gene [KCNH2: potassium ion channel alpha-subunit (Kv11.1) coding gene]
Web source: http://biosig.unimelb.edu.au/pkcsm/

According to Table 5, the total clearance of petunidin is 0.64 ml/min/kg. Furthermore, petunidin is not a substrate of the renal organic cation transporter 2 (OCT2) (Table 5). OCT2 is a renal uptake protein that plays an important role in the regulation and renal clearance of drugs and endogenous compounds. OCT2 substrates may interact adversely with combined OCT2 inhibitors (Pires et al., 2015). The fact that petunidin is not an OCT2 substrate indicates that it does not adversely affect drug excretion processes in the kidney.

According to the pkCSM online server, the estimated AMES test result of petunidin is negative and therefore not mutagenic (Table 5). The maximum recommended tolerated dose (MRTD) provides an estimate of the threshold for toxic doses of chemicals in the human body. According to Table 5, the MRTD of petunidin is 0.52 mg/kg/day, and since this value is greater than 0.477, it was concluded that the MRTD of the petunidin molecule is favorably high. Hopefully, petunidin shows no inhibitory effect on potassium channels encoded by hERG I and hERG II (Table 5). Lethal dose values (LD$_{50}$) are standard values for measuring the relative acute toxicities of different molecules. The rat acute oral toxicity (LD$_{50}$) value for petunidin was calculated as 2.45 mol/kg, and the rat chronic oral toxicity (LOAEL) value was determined as 2.61 log mg/kg.bw/day. These values (LD$_{50}$ and LOAEL) become meaningful when compared with the bioactive concentration of the molecule in the organism and the treatment time, however, in general, highly toxic (positive) chemicals have less than 50 mg/kg (LD$_{50}$ < 50 mg/kg), and non-toxic (negative) chemicals, on the other hand, have

higher than 2000 mg/kg (LD$_{50}$ > 2000 mg/kg) acute oral toxicity values (Gadaleta et al., 2019). In the computational conversion performed according to Table 5, the acute oral toxicity value of petunidin was found to be 778263.31 mg/kg. This value indicates that petunidin is a reliable phytochemical without oral toxicity. Petunidin, promisingly, does not show hepatotoxicity nor does it cause skin sensitization (Table 5). Finally, although petunidin is a potential toxic agent in *Tetrahymena pyriformis* (pIGC$_{50}$ = 0.29 µg/l), it shows no toxic effect in the minnow (LC$_{50}$ = 3.00 log mM).

3.5. Network pharmacology analysis of anthocyanidins

The increase in the rate of drugs failing late in the clinical development process over the last decade stems from the assumption that the goal of drug discovery is to design selective ligands specifically designed for a single disease target. The

underlying assumption of this current drug design approach is that safer, more effective drugs can be obtained through the development of highly selective ligands with eliminated undesirable toxic side effects. However, after nearly two decades of efforts to develop highly selective ligands, the high attrition rate of drugs in the design phase has begun to undermine this hypothesis (Hopkins, 2008; Szklarczyk et al., 2016). Today, the role of the ligand-protein interaction network is even more prominent in the field of drug development, as diseases are often the phenotypic result of multiple changes in the same pathway or multi-protein complex (Barabási et al., 2011; Oti et al., 2006). Taking into account the network in which the individual protein targeted by the ligand is located and the topology of this network can provide a better understanding of the cellular effect of a drug (Hopkins, 2008; Szklarczyk et al., 2016; Yang et al., 2008).
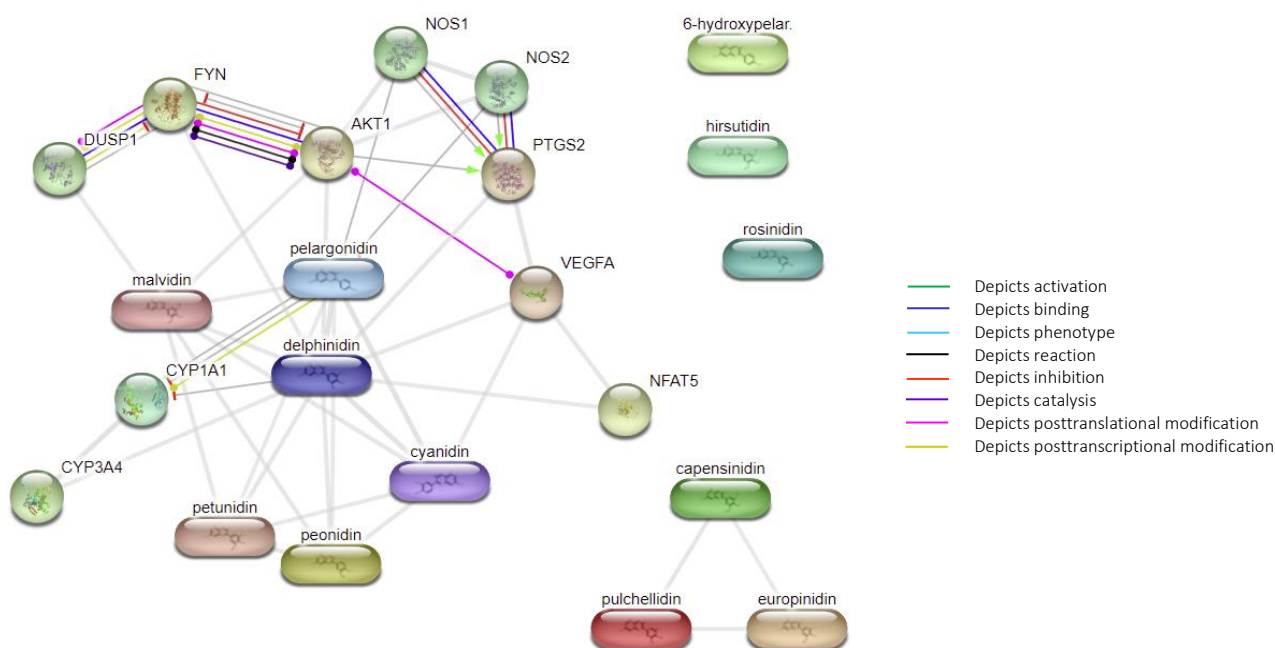

Figure 7. The 'molecular effect' view of the STITCH analysis results showing possible intracellular protein targets and interaction types of twelve anthocyanidin molecules
The minimum interaction score was set as 0.70 (high confidence).
Source: http://stitch.embl.de/cgi/network.pl?taskId=5zMVyBQC4MaY

In this context, the Search Tool for Interactions of Chemicals (STITCH) database was used to determine the interactions of 12 anthocyanidin molecules with their intracellular protein(s) targets and the types of these interactions. The 'minimum required interaction score' was selected as 0.70 (high confidence) in the STITCH server, revealing the possible protein molecular interaction network of anthocyanidins in *H. sapiens* (Figure 7). According to Figure 7, the predicted *H. sapiens* functional protein partners of petunidin, peonidin, cyanidin, delphinidin, malvidin, and pelargonidin appear to be VEGFA, PTGS2, AKT1, NFAT5, FYN, CYP3A4, DUSP1, NOS1, NOS2, and CYP1A1. Furthermore, the anthocyanidins petunidin, peonidin, cyanidin, delphinidin, malvidin, and pelargonidin are highly associated, and delphinidin is at the center of this ligand network (Figure 7). While pelargonidin shows multiple effects such as activation, inhibition, and posttranscriptional regulation (combined score = 0.70) on CYP1A1, delphinidin shows an inhibitory effect (combined score = 0.73) on CYP1A1 protein (Figure 7). Therefore, it can be assumed that there could be a multifunctional interaction between pelargonidin, delphinidin, and CYP1A1. The petunidin molecule, which was determined as the top-ranked ligand in our study, promisingly does

not exert any significant functional interaction with any protein in this molecular interaction network (Figure 7). The molecular interaction network properties for petunidin are also consistent with the ADMET results in Table 5; petunidin does not react in a positive or negative functional manner with any cytochrome P450 enzymes. In previous studies, it has been reported that anthocyanins showed a favorable effect on obesity and diabetes by increasing adipocytokine gene expression and secretion. Cyanidin, but not petunidin, altered the expression levels of this gene in human adipocytes, up-regulated adiponectin and leptin, and induced genes related to lipid metabolism (uncoupling protein 2, acyl-CoA oxidase 1, and perilipin) (Tsuda et al., 2006). Also, cyanidin potentiated the expression of PPAR and adipocyte-specific genes such as adipocyte fatty acid binding protein (aP2) and lipoprotein lipase (LPL) (Tsuda et al., 2004). Although these results do not include the hit ligands identified in our study, a similar mechanism could be suggested for petunidin or other anthocyanidins, since cyanidin is structurally similar to petunidin. In conclusion, these data imply that anthocyanidins may regulate adipocytokine gene expression through multiple mechanisms and provide a preventive effect on obesity and diabetes (Tsuda et al., 2005). However, it should be

noted that different anthocyanidins can affect the expression of different genes.

4. Conclusions

In this study, petunidin, an anthocyanidin phytochemical, showed a very favorable energetic binding potential in molecular docking simulations against human pancreatic α-amylase and intestinal α-glucosidase enzymes (-7.86 kcal/mol for α-amylase; -7.37 kcal/mol for α-glucosidase). The fact that the α-amylase active site is more solvent-accessible and has a large volume was evaluated as a factor that strengthens the interaction of petunidin with this enzyme. It has been determined that the hydrophobic interactions between the aromatic groups (A, C, and B rings) of petunidin and proteins' active site residues are at least as effective as the H-bonds in the interaction of petunidin with human α-amylase and α-glucosidase. According to drug-likeness analysis using the combined Ro5, Ghose, and Veber filters, petunidin showed promising 'hit' molecule properties and strikingly did not violate any physicochemical criteria. ADMET analysis indicated that petunidin was unlikely to be absorbed from the intestinal mucosa and its estimated tissue distribution was poor. On the other hand, petunidin does not interact negatively with liver metabolic enzymes, cytochrome (CYP) P450s, and does not act as a substrate for renal organic cation transporter 2 (OCT2). Very promisingly, petunidin showed no mutagenic potential, and no inhibition on hERG I and hERG II potassium channels, with a reliable LD_{50} profile. Furthermore, network pharmacology analysis showed that petunidin had no negative functional interactions with human intracellular target proteins. Based on molecular docking, drug-likeness, ADMET, and network pharmacology, petunidin can be suggested as a potential α-amylase and α-glucosidase inhibitor in postprandial hyperglycemia observed in T2DM patients. On the other hand, the low gastrointestinal absorption rate should be increased by molecular optimization without compromising petunidin's pharmacological efficacy.

Conflict of interest

The authors confirm that there are no known conflicts of interest.

Statement of ethics

In this study, no method requiring the permission of the "Ethics Committee" was used.

Availability of data and materials

All data generated or analyzed during this study are included in this published article.

CRediT authorship contribution statement

Cihan Demir: Conceptualization, Data curation, Investigation, Methodology, Writing
Erman Salih Istifli: Data curation, Formal analysis, Methodology, Software, Visualization, Review & Editing

ORCID Numbers of the Authors

C. Demir: 0000-0001-7550-2644
E.S. Istifli: 0000-0003-2189-0703

Supplementary File

The supplementary file accompanying this article is available at https://ijpbp.com/index.php/ijpbp/libraryFiles/downloadPublic/10.

References

Barabási, A.L., Gulbahce, N., Loscalzo, J., 2011. Network medicine: a network-based approach to human disease. *Nature Reviews Genetics*, 12(1), 56-68.

Belwal, T., Nabavi, S.F., Nabavi, S.M., Habtemariam, S., 2017. Dietary anthocyanins and insulin resistance: When food becomes a medicine. *Nutrients*, 9(10), 1111.

Carrillo-Larco, R.M., Barengo, N.C., Albitres-Flores, L., Bernabe-Ortiz, A., 2019. The risk of mortality among people with type 2 diabetes in Latin America: A systematic review and meta-analysis of population-based cohort studies. *Diabetes/Metabolism Research and Reviews*, 35(4), e3139.

Castañeda-Ovando, A., de Lourdes Pacheco-Hernández, M., Páez-Hernández, M.E., Rodríguez, J.A., Galán-Vidal, C.A., 2009. Chemical studies of anthocyanins: A review. *Food Chemistry*, 113(4), 859-871.

Chandran, U., Mehendale, N., Tillu, G., Patwardhan, B., 2015. Network pharmacology of ayurveda formulation Triphala with special reference to anti-cancer property. *Combinatorial Chemistry & High Throughput Screening*, 18(9), 846-854.

Chen, J.G., Wu, S.F., Zhang, Q.F., Yin, Z.P., Zhang, L., 2020. α-Glucosidase inhibitory effect of anthocyanins from *Cinnamomum camphora* fruit: Inhibition kinetics and mechanistic insights through *in vitro* and *in silico* studies. *International Journal of Biological Macromolecules*, 143, 696-703.

Chen, L., Magliano, D.J., Zimmet, P.Z., 2012. The worldwide epidemiology of type 2 diabetes mellitus—present and future perspectives. *Nature Reviews Endocrinology*, 8(4), 228-236.

Coman, C., Rugina, O.D., Socaciu, C., 2012. Plants and natural compounds with antidiabetic action. *Notulae Botanicae Horti Agrobotanici Cluj-Napoca*, 40(1), 314-325.

Congreve, M., Carr, R., Murray, C., Jhoti, H., 2003. A'rule of three'for fragment-based lead discovery?. *Drug Discovery Today*, 8(19), 876-877.

Daina, A., Michielin, O., Zoete, V., 2017. SwissADME: a free web tool to evaluate pharmacokinetics, drug-likeness and medicinal chemistry friendliness of small molecules. *Scientific Reports*, 7(1), 1-13.

Daina, A., Michielin, O., Zoete, V., 2019. SwissTargetPrediction: updated data and new features for efficient prediction of protein targets of small molecules. *Nucleic Acids Research*, 47(W1), W357-W364.

Delaney, J.S., 2004. ESOL: estimating aqueous solubility directly from molecular structure. *Journal of Chemical Information and Computer Sciences*, 44(3), 1000-1005.

Finch, A., Pillans, P., 2014. P-glycoprotein and its role in drug-drug interactions. *Australian Prescriber*, 37(4), 137-139.

Forouhi, N.G., Wareham, N.J., 2014. Epidemiology of diabetes. *Medicine (Abingdon)*, 42 (12): 698–702.

Gadaleta, D., Vuković, K., Toma, C., Lavado, G.J., Karmaus, A.L., Mansouri, K., Roncaglioni, A., 2019. SAR and QSAR modeling of a large collection of LD_{50} rat acute oral toxicity data. *Journal of Cheminformatics*, 11(1), 1-16.

Ghose, A.K., Viswanadhan, V.N., Wendoloski, J.J., 1999. A knowledge-based approach in designing combinatorial or medicinal chemistry libraries for drug discovery. 1. A qualitative and quantitative characterization of known drug databases. *Journal of Combinatorial Chemistry*, 1(1), 55-68.

Gleeson, M.P., 2008. Generation of a set of simple, interpretable ADMET rules of thumb. *Journal of Medicinal Chemistry*, 51(4), 817-834.

Hann, M.M., Keserü, G.M., 2012. Finding the sweet spot: the role of nature and nurture in medicinal chemistry. *Nature Reviews Drug Discovery*, 11(5), 355-365.

Hopkins, A.L., 2008. Network pharmacology: the next paradigm in drug discovery. *Nature Chemical Biology*, 4(11), 682-690.

Horbowicz, M., Kosson, R., Grzesiuk, A., Debski, H., 2008. Anthocyanins of fruits and vegetables-their occurrence, analysis and role in human nutrition. *Vegetable Crops Research Bulletin*, 68, 5-22.

Iacobucci, G.A., Sweeny, J.G., 1983. The chemistry of anthocyanins, anthocyanidins and related flavylium salts. *Tetrahedron*, 39(19), 3005-3038.

Istifli, E.S., Netz, P.A., Sihoglu Tepe, A., Husunet, M.T., Sarikurkcu, C., Tepe, B., 2022. *In silico* analysis of the interactions of certain flavonoids with the receptor-binding

domain of 2019 novel coronavirus and cellular proteases and their pharmacokinetic properties. *Journal of Biomolecular Structure and Dynamics*, 40(6), 2460-2474.

Jayawardena, R., Ranasinghe, P., Galappatthy, P., Malkanthi, R.L.D.K., Constantine, G.R., Katulanda, P., 2012. Effects of zinc supplementation on diabetes mellitus: a systematic review and meta-analysis. *Diabetology & Metabolic Syndrome*, 4(1), 1-12.

Kell, D.B., Dobson, P.D., Oliver, S.G., 2011. Pharmaceutical drug transport: the issues and the implications that it is essentially carrier-mediated only. *Drug Discovery Today*, 16(15-16), 704-714.

Khoo, H.E., Azlan, A., Tang, S.T., Lim, S.M., 2017. Anthocyanidins and anthocyanins: Colored pigments as food, pharmaceutical ingredients, and the potential health benefits. *Food & Nutrition Research*, 61(1), 1361779.

Krasiński, A., Radić, Z., Manetsch, R., Raushel, J., Taylor, P., Sharpless, K.B., Kolb, H.C., 2005. *In situ* selection of lead compounds by click chemistry: target-guided optimization of acetylcholinesterase inhibitors. *Journal of the American Chemical Society*, 127(18), 6686-6692.

Lipinski, C.A., Lombardo, F., Dominy, B.W., Feeney, P. J. (2012). Experimental and computational approaches to estimate solubility and permeability in drug discovery and development settings. *Advanced Drug Delivery Reviews*, 64, 4-17.

Liu, Y., Wang, Q., Wu, K., Sun, Z., Tang, Z., Li, X., Zhang, B., 2022. Anthocyanins' effects on diabetes mellitus and islet transplantation. *Critical Reviews in Food Science and Nutrition*, 1-24.

Lobo, S., 2020. Is there enough focus on lipophilicity in drug discovery?. *Expert Opinion on Drug Discovery*, 15(3), 261-263.

Malde, A.K., Zuo, L., Breeze, M., Stroet, M., Poger, D., Nair, P.C., Mark, A.E., 2011. An automated force field topology builder (ATB) and repository: version 1.0. *Journal of Chemical Theory and Computation*, 7(12), 4026-4037.

Meng, X.Y., Zhang, H.X., Mezei, M., Cui, M., 2011. Molecular docking: a powerful approach for structure-based drug discovery. *Current Computer-Aided Drug Design*, 7(2), 146-157.

Oliveira, H., Fernandes, A., Brás, N., Mateus, N., de Freitas, V., Fernandes, I., 2020. Anthocyanins as antidiabetic agents—*in vitro* and *in silico* approaches of preventive and therapeutic effects. *Molecules*, 25(17), 3813.

Oti, M., Snel, B., Huynen, M.A., Brunner, H.G., 2006. Predicting disease genes using protein–protein interactions. *Journal of Medical Genetics*, 43(8), 691-698.

Pedretti, A., Villa, L., Vistoli, G., 2004. VEGA–an open platform to develop chemo-bio-informatics applications, using plug-in architecture and script programming. *Journal of Computer-Aided Molecular Design*, 18(3), 167-173.

Pellecchia, M., Becattini, B., Crowell, K.J., Fattorusso, R., Forino, M., Fragai, M., Tautz, L., 2004. NMR-based techniques in the hit identification and optimisation processes. *Expert Opinion on Therapeutic Targets*, 8(6), 597-611.

Pérez Gutierrez, R., Hernández Luna, H., Hernández Garrido, S., 2006. Antioxidant activity of *Tagetes erecta* essential oil. *Journal of the Chilean Chemical Society*, 51(2), 883-886.

Peterson, J.J., Dwyer, J.T., Jacques, P.F., McCullough, M.L., 2015. Improving the estimation of flavonoid intake for study of health outcomes. *Nutrition Reviews*, 73(8), 553-576.

Pires, D.E., Blundell, T.L., Ascher, D.B., 2015. pkCSM: predicting small-molecule pharmacokinetic and toxicity properties using graph-based signatures. *Journal of Medicinal Chemistry*, 58(9), 4066-4072.

Promyos, N., Temviriyanukul, P., Suttisansanee, U., 2020. Investigation of anthocyanidins and anthocyanins for targeting α-glucosidase in diabetes mellitus. *Preventive Nutrition and Food Science*, 25(3), 263-271.

Sanner, M.F., 1999. Python: a programming language for software integration and development. *Journal of Molecular Graphics and Modelling*, 17(1), 57-61.

Santos, R.N.D., Ferreira, L.G., Andricopulo, A.D., 2018. Practices in molecular docking and structure-based virtual screening. In Computational drug discovery and design (pp. 31-50). Humana Press, New York, NY.

Sharma, S. (1996). Applied multivariate techniques. Wiley, ISBN: 978-0-471-31064-8.

Shultz, M.D., 2018. Two decades under the influence of the rule of five and the changing properties of approved oral drugs: miniperspective. *Journal of Medicinal Chemistry*, 62(4), 1701-1714.

Sivamaruthi, B.S., Kesika, P., Subasankari, K., Chaiyasut, C., 2018. Beneficial effects of anthocyanins against diabetes mellitus associated consequences-A mini review. *Asian Pacific Journal of Tropical Biomedicine*, 8(10), 471-477.

Sky-Peck, H.H., Thuvasethakul, P., 1977. Human pancreatic alpha-amylase. II. Effects of pH, substrate and ions on the activity of the enzyme. *Annals of Clinical & Laboratory Science*, 7(4), 310-317.

Szklarczyk, D., Santos, A., Von Mering, C., Jensen, L.J., Bork, P., Kuhn, M., 2016. STITCH 5: augmenting protein–chemical interaction networks with tissue and affinity data. *Nucleic Acids Research*, 44(D1), D380-D384.

Testa, B., Vistoli, G., Pedretti, A., van de Waterbeemd, H., Avdeef, A., Ivanciuc, O., Muresan, S., 2007. Molecular drug properties: measurement and prediction. Wiley, ISBN:9783527621286.

Tomasik, P., Horton, D., 2012. Enzymatic conversions of starch. *Advances in Carbohydrate Chemistry And Biochemistry*, 68, 59-436.

Trott, O., Olson, A.J., 2010. AutoDock Vina: improving the speed and accuracy of docking with a new scoring function, efficient optimization, and multithreading. *Journal of Computational Chemistry*, 31(2), 455-461.

Tsuda, T., Ueno, Y., Aoki, H., Koda, T., Horio, F., Takahashi, N., Osawa, T., 2004. Anthocyanin enhances adipocytokine secretion and adipocyte-specific gene expression in isolated rat adipocytes. *Biochemical and Biophysical Research Communications*, 316(1), 149-157.

Tsuda, T., Ueno, Y., Kojo, H., Yoshikawa, T., Osawa, T., 2005. Gene expression profile of isolated rat adipocytes treated with anthocyanins. *Biochimica et Biophysica Acta (BBA)-Molecular and Cell Biology of Lipids*, 1733(2-3), 137-147.

Tsuda, T., Ueno, Y., Yoshikawa, T., Kojo, H., Osawa, T., 2006. Microarray profiling of gene expression in human adipocytes in response to anthocyanins. *Biochemical Pharmacology*, 71(8), 1184-1197.

Veber, D.F., Johnson, S.R., Cheng, H.Y., Smith, B.R., Ward, K.W., Kopple, K.D., 2002. Molecular properties that influence the oral bioavailability of drug candidates. *Journal of Medicinal Chemistry*, 45(12), 2615-2623.

Vistoli, G., Pedretti, A., Testa, B., 2008. Assessing drug-likeness–what are we missing?. *Drug Discovery Today*, 13(7-8), 285-294.

Wallace, T.C., Giusti, M.M., 2015. Anthocyanins. *Advances in Nutrition*, 6(5), 620-622.

Wiernsperger, N., Rapin, J., 2010. Trace elements in glucometabolic disorders: an update. *Diabetology & Metabolic Syndrome*, 2(1), 1-9.

Yang, K., Bai, H., Ouyang, Q., Lai, L., Tang, C., 2008. Finding multiple target optimal intervention in disease-related molecular network. *Molecular Systems Biology*, 4(1), 228.

Zamora-Ros, R., Knaze, V., Luján-Barroso, L., Slimani, N., Romieu, I., Fedirko, V., González, C.A., 2011. Estimated dietary intakes of flavonols, flavanones and flavones in the European Prospective Investigation into Cancer and Nutrition (EPIC) 24 hour dietary recall cohort. *British Journal of Nutrition*, 106(12), 1915-1925.

Zhang, J., Sun, L., Dong, Y., Fang, Z., Nisar, T., Zhao, T., Guo, Y., 2019. Chemical compositions and α-glucosidase inhibitory effects of anthocyanidins from blueberry, blackcurrant and blue honeysuckle fruits. *Food Chemistry*, 299, 125102.

Zheng, Y., Ley, S.H., Hu, F.B., 2018. Global aetiology and epidemiology of type 2 diabetes mellitus and its complications. *Nature Reviews Endocrinology*, 14(2), 88-98.

Reviewed by: